XVII IMEKO World Congress
Metrology in the 3rd Millennium
June 22–27, 2003, Dubrovnik, Croatia

A VISION SYSTEM FOR ONLINE WEAR DETECTION

Jianbo Zhang, Maarten Korsten, Paul Regtien

Department of Electrical Engineering, University of Twente, Enschede, the Netherlands

Abstract – Wear detection has traditionally restricted itself to offline study and measurement. In this paper a vision system for online monitoring and detection of wear is described. This system uses a video zoom microscope and a high-resolution monochrome camera to capture the image series of a moving surface under study. An algorithm based on multichannel filtering for the detection of wear patterns is presented. The wear patterns are extracted by filtering the acquired image using a Gabor filter bank with multiple narrow spatial frequency and orientation channels. Experiments show the feasibility and usefulness of the proposed vision system and detection method of wear patterns.

Keywords: Online wear detection

1. INTRODUCTION

Wear is one of the main causes of replacement of key machinery elements in their every aspect of life. Detection and monitoring of wear, therefore, is very important not only in studying material properties but also in predicting the lifetime of product components and guaranteeing their reliability and effectiveness. Traditional methods of the measurement of wear are often based on the measurement of mass differences, volume differences, or displacements generated by wear [7]. Using these methods global information about wear can be obtained. Local information, however, is more helpful and valuable since wear takes place at a microscopic scale between contacting asperities of the surfaces in contact.

The surface profile has a big influence on the tribological properties and service life of machine elements. Therefore, measurement of profile changes of finished or worn surfaces is frequently carried out in engineering and research [1, 2]. Several techniques of microscopy, such as interference microscopy, atomic force microscopy, scanning tunnelling microscopy, and so on, are extensively used to obtain surface topography [4]. Although these profiling techniques have high depth resolution, down to nanometers, they have some weak points. First, these techniques can only measure wear offline. During the experiment, the specimen must be removed from the tester periodically to measure the evolution of wear as a function of time or sliding distance. It is very difficult to re-measure at the same location on the specimen before and after the wear test. The mounting and dismounting steps unavoidably bring in errors. Second, the measurement using these techniques is very sensitive to vibrations. Besides, light sectioning and grating projection based approaches also can be used to obtain the surface profile [8], but they have relatively poor lateral resolution and are not suitable for measuring surfaces in motion as well.

In tribology research and some practical applications, timely detection and quantification of wear online is required. Online wear detection, compared with the conventional offline methodology, is more accurate and significant in the sense of neither interrupting the dynamic process of wear nor changing the wear condition. Therefore, this approach is possibly useful for the investigation of a particular wear mechanism and practical surface inspection.

In the WEAR project sponsored by STW (Dutch Technology Foundation), studies of noncontact detection and monitoring of micro- and macrowear using imaging methods are currently being carried out. One of the aims of this project is to develop online methodologies for the detection and monitoring of wear. A simple vision system for this purpose is currently developed.

A computer-based vision system is a good strategy for non-contact, online, and high speed wear detection and monitoring. It is suitable for applications in an automated environment, where high speed and low cost are required. It also allows one to visualize and gain further understanding of the wear process by viewing the time series of photomicrographs. The composition of this vision system will be described in detail in subsection 2.1. Using this vision system a sequence of photomicrographs of the surface of the specimen under test is captured and filtered by a Gabor filter bank with multiple narrow spatial frequency and orientation channels. By this way, the wear patterns with different sizes and orientations, which occur on the surface, are extracted. The changes of these detected wear patterns indicate the wear status of the specimen being monitored. The procedure of the extraction of wear patterns is addressed in subsection 2.3. The experimental results and discussions will be given in subsection 2.4 followed by conclusions as well as future work in section 3.

2. ONLINE WEAR DETECTION TECHNIQUE

Modern fabrication of parts typically involves machining, grinding, and polishing to remove material and to create a surface with specific macroscopic dimensions and also microscopic roughness. One of the purposes of this

process is to reduce the risk of suffering wear during the surface use. Most surfaces appear as regular textures to a certain extent due to the quasi-periodical process of surface fabrication. Fig. 1 shows an example of a surface image of stainless steel manufactured by turning operation. From this image one can see approximately parallel strips, corresponding to grooves or lays in a real surface.

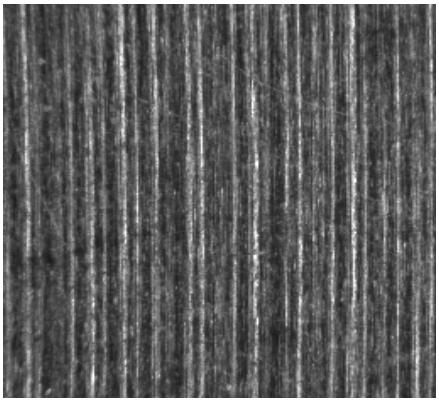

Fig. 1. A surface image of stainless steel fabricated by turning

When a beam of light is reflected by a rough surface, the intensity and pattern of the scattered radiation depend on the roughness heights, the spatial wavelengths of the surface and the wavelength of the light [4]. In the case of one textured surface sliding upon another one, the surface with softer material wears and its worn area becomes smoother as the asperities are removed. This will result in apparent texture changes in the images (see Fig. 6b) captured by a properly designed vision system, which will be described in detail in the following subsection. As a consequence, the worn regions of the surface, referred to as wear patterns in images, can be characterised as texture changes with respect to the unworn region. The area and orientation of wear patterns indicate the wear state of the surface. Thus, wear detection and characterization can be carried out, using an image texture analysis process.

2.1. Experimental set-up

A schematic diagram of the experimental set-up is shown in Fig. 2. A wear test is conducted by loading a flat or sphere shaped indenter, pin or ball, which is mounted on a stiff lever, onto a test sample that is fixed on a motor-driven rotary table. A servo motor controller is used to vary the rotation speed of the table. The load applied on the test sample is controlled by removing or adding weights on the lever. The surface of the test sample is ground or machined. The indenter made of harder material is used to evoke wear on the sample.

The wearing surface is monitored by a vision system, which is a combination of a video zoom microscope and a monochrome CCD sensor. The magnification of the imaging system is 2.5× to 10×; the corresponding system resolution (lateral) is 9.8 to 4.4 μm. The optical axis of the system is perpendicular to the nominal plane of the test surface. Image sequences are captured through a frame grabber into a computer in real time. A 150-watt fiber optic illuminator, through a ring guide that is mounted at the end of the microscope, provides glare-free and heat-free illumination for the system. The intensity can be adjusted manually.

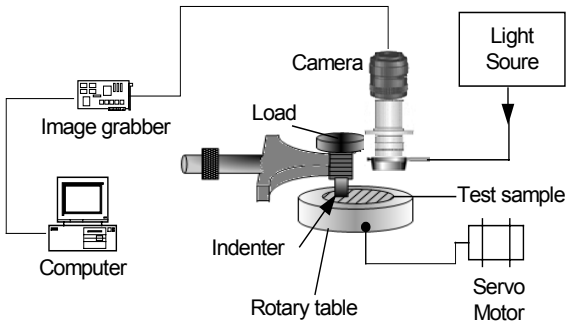

Fig. 2. Schematic diagram of the experimental set-up

2.2. Gabor filter bank

As explained at the beginning of this section, the area and orientation of wear patterns give the clues of the wear state of the surface being monitored. In this subsection we will address how to extract wear patterns from textured images, which is actually a texture interpretation and a segmentation problem.

There are a lot of approaches to texture segmentation. Two well-known categories among them are statistical, and filtering approaches. The gray level co-occurrence matrix, belonging to the statistical methods, is very computation consuming [10] and sensitive to image quality, and therefore is not suitable for online wear detection. As to the filtering approach, Fourier-domain-based techniques are particularly suitable for materials that exhibit high degree of periodicity. But Fourier analysis does not provide, in general, enough information on local features. Methods that can localize features in the spatial as well as in the frequency domain are convenient for detecting local wear patterns. As Gabor filters yield optimal localization in space and frequency domains [6], they are extensively used for texture analysis [3, 5], and are also adopted in this paper to extract wear patterns occurring on textured surfaces. Next a brief introduction about Gabor filters is given.

In the spatial domain, the Gabor function is a complex exponential modulated by a Gaussian function. It has the following general form [3, 5]:

$$g(x,y)=\frac{1}{2\pi\sigma_x\sigma_y}\exp[-\frac{1}{2}(\frac{x^2}{\sigma_x^2}+\frac{y^2}{\sigma_y^2})+2\pi j u_0 x] \qquad (1)$$

where u_0 denotes the radial frequency of the Gabor function, σ_x and σ_y the standard deviation of the Gaussian envelope. In the frequency domain, the Gabor function acts as a band-pass filter and its Fourier transform is:

$$G(u,v)=\exp\{-\frac{1}{2}[\frac{(u-u_0)}{\sigma_u^2}+\frac{v^2}{\sigma_v^2}]\} \qquad (2)$$

where $\sigma_u=1/2\pi\sigma_x$, $\sigma_v=1/2\pi\sigma_y$. A self-similar filter bank can be obtained by appropriate dilation and rotation of

$g(x, y)$ through the generating function

$$g_{mn}(x, y) = \alpha^{-m} g(x', y') \quad (3)$$

where $x' = \alpha^{-m}(x\cos\theta + y\sin\theta)$, $y' = \alpha^{-m}(-x\sin\theta + y\cos\theta)$, $\alpha > 1$, $m = 1, 2, \ldots, P$, $n = 1, 2, \ldots, Q$, $\theta = (n\text{-}1)\pi/Q$, P and Q are the total number of scales and orientations respectively.

The parameters of the Gabor filter bank, α, σ_x and σ_y are selected as illustrated in [3] to ensure that the half-peak magnitude responses of adjacent filters touch each other to reduce redundancy. In [5] the real and imaginary part of each of the complex Gabor functions are used for filtering. In our case, experiments show that the imaginary part does not provide further improvement for the extraction of wear patterns. For this reason, only the real part of the Gabor function is adopted, i.e., (1) is replaced with

$$g(x, y) = \frac{1}{2\pi\sigma_x\sigma_y}\exp[-\frac{1}{2}(\frac{x^2}{\sigma_x^2} + \frac{y^2}{\sigma_y^2})]\cos(2\pi u_0 x) \quad (4)$$

Using only the real part also greatly saves computational load.

2.3. Wear pattern extraction

The procedure of wear pattern extraction is illustrated in Fig. 3:

a. *Enhancing the input image to emphasize and sharpen the image features for further analysis.*

As the gray level intensities of the images under wear detection is directly related to the extent of wear on the surface, the enhancement should not re-distribute the gray values. Here histogram stretching is applied:

$$I(x,y)_{str} = \frac{I(x,y) - I(x,y)_{MIN}}{I(x,y)_{MAX} - I(x,y)_{MIN}}(MAX - MIN) + MIN \quad (5)$$

where $I(x,y)_{MIN}$ and $I(x,y)_{MAX}$ are the minimum and maximum gray values in the image. *MAX* and *MIN* correspond to the maximum and the minimum gray levels in the enhanced images. Histogram stretching would result in an image with a higher contrast, which is particularly useful when the pixel values fall within a small range.

b. *Filtering the enhanced image using the Gabor filter bank (3), which allows multiresolution analysis of image texture.*

Each of the Gabor functions can be implemented as a spatial mask of size N×N (see Fig. 5). For a given input image $I(x, y)$, the magnitude of the filtered image $I_{mn}(x, y)$ is obtained by using the Gabor filter function $g_{mn}(x, y)$ as follows:

$$I_{mn}(x, y) = | I_{str}(x, y) * g_{mn}(x, y) | \quad (6)$$

where "*" denotes 2-D convolution. Namely, the image is filtered by each channel that is tuned to a narrow range of size and orientation. The filtered images from different channels are called feature images. The same operation is also applied to a wear-free reference image to get reference feature images, which are used to compute feature difference images for recognizing wear features. The reference feature images are computed at the beginning of the wear detection as a calibration operation, which does not increase computational load in the online detection.

c. *Computing the feature difference images and fusing them to be a unique feature image.*

Each feature image $I_{mn}(x, y)$ obtained in the previous step is compared with each corresponding reference feature image to compute the feature difference image, in which only possible wear features are remained. In addition, as the information gathered by different channels is often uncertain, fuzzy or incomplete, it is better to fuse all the feature difference images. Experiments show that the approach proposed in [5] for feature difference and data fusion is fast and also works well in our case, therefore is adopted as well.

d. *Thresholding the fused image to suppress the pixels not belonging to wear patterns*

To separate the wear patterns and further reducing the probability of false alarm, a thresholding operation is applied. From the histogram of the fused image (see Fig. 4) one can find two peaks, each peak belonging to one class (the left peak to background noise, the right peak to wear patterns). For this histogram shape, the best threshold value to separate the wear patterns can be found by using an automatic isodata thresholding procedure [9].

Through the procedure above, wear patterns with different sizes and orientations are successfully extracted. Important wear features such as wear area, centroid, area moments and products of inertia, wear orientation, and so on can be calculated from the separated wear patterns to indicate wear state of the surface being monitored.

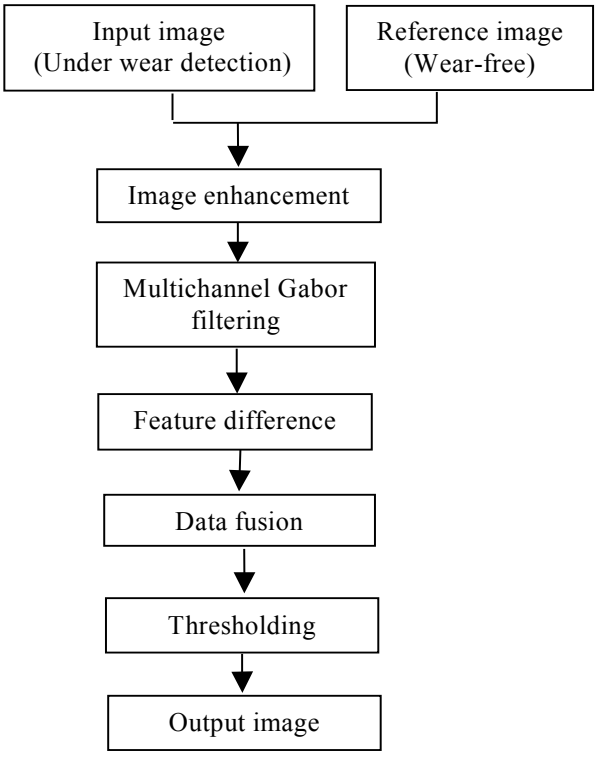

Fig. 3. Schematic diagram of wear pattern extraction procedure

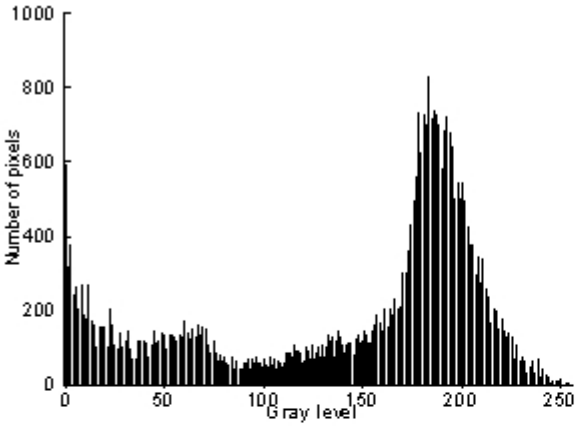

Fig. 4. Histogram of a fused image before thresholding

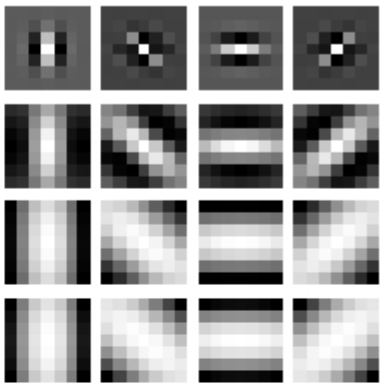

Fig. 5. 4 × 4 real Gabor filters in spatial domain

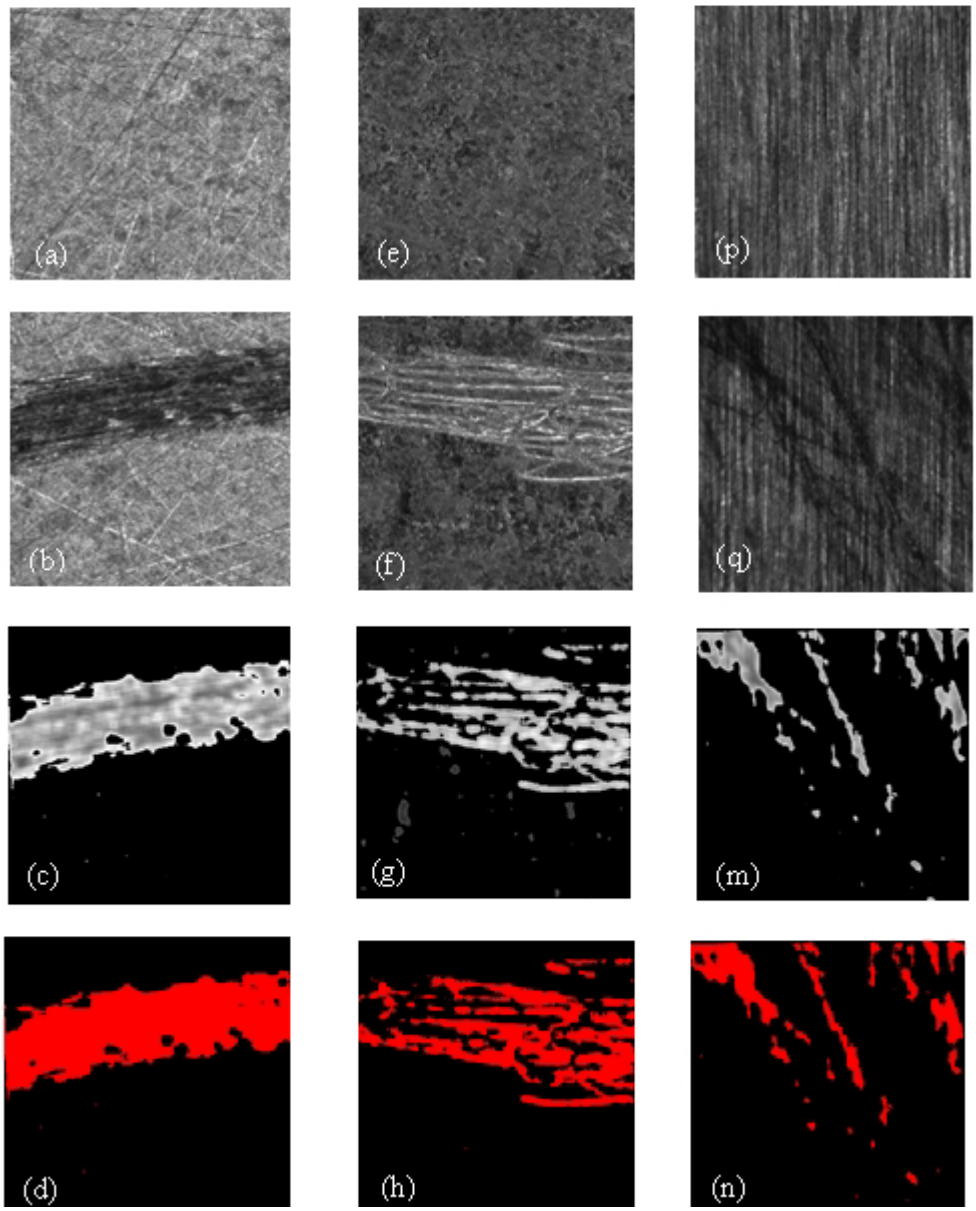

Fig. 6. Samples with wear: reference images of the samples in (a), (e) , (p) ; images of the samples with wear in (b), (f), (q); corresponding filtered images in (c), (g), (m); segmented wear patterns in (d), (h), (n).

2.4. Results and discussions

The performance of the vision system for online wear detection using the multichannel filtering scheme described above was evaluated on three test samples with different surface textures. One is a machined steel ring with a wear track in the middle (Fig. 6b), the second is a vapor-polished aluminium bar with wear scratches (Fig. 6f), the third one is a ground steel bar with wear scratches (Fig. 6q).

In the experiment, a bank of 4 × 4 Gabor filters described in subsection 2.2 are adopted for detection of wear patterns. Each Gabor filter is implemented as a spatial 7 × 7 mask for a computational compromise. A small mask size corresponds to small computation load, which is desirable for online wear detection. The frequency range of Gabor filters in the filter bank depends on the range of wear patterns to be detected. Fig. 5 shows the representation of the Gabor bank using 7 × 7 masks in the spatial domain.

The experimental results are shown in Fig. 6, of which the top row (Figs. 6a, 6e and 6p) are wear-free images captured during the calibration phase; the second row (Figs. 6b, 6f and 6q) are images acquired during wear processes; the third row (Figs. 6c, 6g and 6m) are images after multichannel filtering and fusion operation; the bottom row (Figs. 6d, 6h and 6n) shows the segmented wear patterns (red colour-coded regions). From these experiments one can find that, using the proposed multichannel filtering algorithm, the wear patterns (wear scratches or wear track) occurring on the surfaces of the three samples are successfully extracted. As mentioned previously, from these separated wear patterns, some wear features, such as their shape (area and orientation), centroid, moments and products of inertia, length of principal axes, etc. can be further calculated to indicate wear state of the surface being monitored.

It is seen that using the simple vision system to detect and monitor wear makes it possible to overcome or reduce concerns about repositioning errors, sensitivity to vibrations, slow measurement speed and additional damages to surfaces in offline methods, irrespective contact or noncontact, etc. Unfortunately, it also has restrictions. First of all, it is only suitable for monitoring clean surfaces. The presence of contaminant or non-transparent lubricant will result in errors. Secondly, the surface being monitored must be very smooth because the microscope easily gets out of focus when surface roughness is large, due to its small depth of focus especially at high magnification. Thirdly, this approach is only useful for detecting the initial and moderate stage of a wear process because with the wear process further going on, surface changes in depth will dominate changes in spatial direction.

3. CONCLUSIONS AND FUTUR WORK

This paper presents a new approach to detect and monitor microwear online using a vision system. Multichannel filtering using a Gabor filter bank is suitable for extracting wear patterns on textured surfaces machined with different methods. This approach is feasible in detecting dry sliding wear especially at the initial and moderate wear stage.

So far extraction of wear patterns using the vision system is investigated. The future work is to study the correlation between changes of wear features and wear rate of a specific surface.

REFERENCES

[1] S. Yin, J. Li, M. Song, “Surface profile measurement using a unique microtube-based system”, *Opt. Comm.,* vol. 168, pp. 1-6, 1999.

[2] R. Gahlin, S. Jacobson, “ A novel method to map and quantify wear on a micro-scale”, *Wear,* vol. 222, pp. 93-102, 1998.

[3] B. S. Manjunath and W. Y. Ma, “Texture features for browsing and retrieval of image data”, *IEEE Trans. Pattern Anal. Machine Intell.,* vol. 18, no. 8, pp. 837-842, 1996

[4] T. R. Thomas, “ Rough Surface”, *Imperial College Press,* 1999.

[5] A. Kumar, G. K. H. Pang, “Defect detection in textured materials using Gabor filters”, *IEEE Trans. Ind. Applicat.*, vol. 38, no. 2, pp. 425-439.

[6] J. G. Daugman, “Uncertainty relation for resolution in space, spatial frequency and orientation optimised by two dimensional visual cortical filters”, *J. Opt. Soc. Am.*, vol. 2, no. 7, pp. 1160-1169, 1985.

[7] M. B. de Rooij, “Tribological aspects of unlubricated deepdrawing process”, *Ph.D. thesis*, *University of Twente*, 1998.

[8] M. B. Kiran, B. Ramamoorthy, V. Radhakrishnan, “ Evaluation of surface roughness by vision system”, Int. J. Mach. Tools Manufact. vol. 38, nos 5-6, pp. 685-690, 1998.

[9] http://www.ph.tn.tudelft.nl/Courses/FIP/noframes/fip-Segmenta.html.

[10] David A. Clausi, “Comparison and fusion of co-occurrence, Gabor and MRF texture features for classification of SAR sea-ice imagery”, *Atomospere-Ocean,* vol. 39, no.3, pp. 183-194, 2001.

Authors: Jianbo Zhang, Maarten Korsten, Paul Regtien, are with the Lab. for Measurement and Instrumentation, Department of Electrical Engineering, P.O. Box 217, 7500 AE, Enschede, the Netherlands; Phone: +31 53 489 2778; Fax: +31 53 489 1067; Email: {j.b.zhang; m.j.korsten; p.p.l.regtien} @el.utwente.nl